

Interpretation and Quantification of Magnetic Interaction through Spin Topology

Satadal Paul and Anirban Misra*

Department of Chemistry, University of North Bengal, Siliguri, PIN 734 013, West Bengal, India

S Supporting Information

ABSTRACT: This work develops a formalism to quantify the interaction among unpaired spins from the ground state spin topology. Magnetic systems where the spins are coupled through direct exchange and superexchange are chosen as references. Starting from a general Hamiltonian, an effective Hamiltonian is obtained in terms of spin density which is utilized to compute exchange coupling constants in magnetic systems executing direct exchange. The high-spin–low-spin energy gap, required to extract the coupling constant, is obtained through the broken symmetry approach within the framework of density functional theory. On the other hand, a perturbative approach is adopted to address the superexchange process. Spin transfer in between the sites in the exchange pathway is found to govern the magnetic nature of a molecule executing superexchange. The metal–ligand magnetic interaction is estimated using the second order perturbation energy for ligand to metal charge transfer and spin densities on the concerned sites. Using the present formalism, the total coupling constant in a superexchange process is also partitioned into the contributions from metal–ligand and metal–metal interactions. Sign and magnitude of the exchange coupling constants, derived through the present formalism, are found to be in parity with those obtained using the well-known spin projection technique. Moreover, in all of the cases, the ground state spin topology is found to complement the sign of coupling constants. Thus, the spin topology turns into a simple and logical means to interpret the nature of exchange interaction. The spin density representation in the present case resembles McConnell’s spin density Hamiltonian and in turn validates it.

■ INTRODUCTION

Magnetism is induced in a material through the coupling of its inherent spin moments. There exists a miscellany of exchange mechanisms such as direct exchange, indirect exchange, double exchange, superexchange, and so on, through which the spins can interact. A rigorous analysis of this exchange interaction is a prerequisite for a clear understanding of the magnetic nature of any system. However, irrespective of their mechanisms, the exchange interactions are usually quantified through the phenomenological Heisenberg–Dirac–van Vleck (HDDVV) spin Hamiltonian:

$$\hat{H} = - \sum_{i < j} J_{ij} \hat{S}_i \cdot \hat{S}_j \quad (1)$$

where, \hat{S}_i and \hat{S}_j are the spin angular momentum operators on magnetic sites i and j and J_{ij} is the exchange coupling constant between them. Since, this Hamiltonian is simply related to spin eigenfunctions, it becomes necessary to map the eigenvalues and eigenfunctions of an exact nonrelativistic Hamiltonian into this HDDVV Hamiltonian. Moreira and Illas have shown that for an interaction between two spin-1/2 sites, it is possible to map the Heisenberg eigenstates to the triplet and singlet N -electron states, and the coupling constant can be derived from the singlet–triplet energy difference.¹ However, sometimes the energy difference is equated with twice the exchange integral because of the occasional appearance of an extra factor of 2 in the Heisenberg Hamiltonian.² The intersite magnetic coupling is found to originate from local electronic interaction between two specific magnetic sites.³ This opens up the possibility of accurate estimation of spin state energies and hence J , using ab initio methods. In fact, different ab initio

multireference configuration interaction (MRCI) tools have been found effective in producing the desired degree of accuracy,⁴ among which the difference dedicated CI (DDCI) approach by Miralles et al. has been particularly successful.⁵ Different variants of the DDCI wave function have also been formulated which can account for second order mechanisms such as double spin polarization, kinetic exchange, etc.⁶ Another ab initio technique, complete active space second-order perturbation theory (CASPT2), is also found useful in producing J value close to DDCI or experimental values.⁷ Compared to these computationally demanding ab initio techniques for the estimation of J , the density functional theory (DFT) based approaches have emerged as the best compromise between computational rigor and accuracy.⁸ In this DFT framework, one can relate J to the energy difference between the high spin ferromagnetic (FM) and the broken symmetry (BS) solution for open shell singlet. This BS approach, primarily proposed by Noodleman, makes use of an unrestricted or spin polarized formalism.⁹ However, the main limitation with DFT has been the proper choice of exchange correlational (XC) functional during the estimation of any electronic property.¹⁰ The value of the coupling constant is also found to be sensitive toward the percentage of Fock exchange on the XC functional.¹¹ Zhao and Truhlar have developed a suite of M06 functionals which bear the facility to change the fraction of HF exchange from 0 to 100%.¹² Among four different functionals of this suite, M06, which contains 27% HF exchange, produces a J value closer to the experimental value.¹³ Not only the exchange effect but also the electron

Received: September 16, 2011

Published: January 24, 2012



correlation effects play a crucial role in describing the magnetic coupling. To confront the short-range and long-range inter-electronic interaction, another new suite of range separated functionals has been introduced by Scuseria and co-workers.¹⁴ Regarding the estimation of J , long-range corrected range separated hybrids appear to be the better performers compared to usual hybrid functionals.^{14a,b} The coupling constant also shows sensitivity to the range separation parameter in the weight function of the range separated hybrids.^{14c} Apart from the selection of a proper XC functional, the unrestricted formalism used in DFT brings about an additional problem of spin contamination, particularly in the BS state.¹⁵ To avoid this, usually the following spin-projected methods are adopted:^{9,16}

$$\begin{aligned} J_{\text{GND}} &= \frac{E_{\text{BS}}^{\text{DFT}} - E_{\text{HS}}^{\text{DFT}}}{S_{\text{max}}^2} \\ J_{\text{BR}} &= \frac{E_{\text{BS}}^{\text{DFT}} - E_{\text{HS}}^{\text{DFT}}}{S_{\text{max}}(S_{\text{max}} + 1)} \\ J_{\text{Y}} &= \frac{E_{\text{BS}}^{\text{DFT}} - E_{\text{HS}}^{\text{DFT}}}{\langle S^2 \rangle_{\text{HS}} - \langle S^2 \rangle_{\text{BS}}} \end{aligned} \quad (2)$$

The applicability of the above equations depends upon the degree of overlap between the magnetic orbitals. Ginsberg, Noodleman, and Davidson derived J_{GND} in case of a weak overlap between magnetic orbitals. This is further modified by Bencini and Ruiz to get J_{BR} which describes the situation of strong overlap between magnetic orbitals. However, the third of this series, J_{Y} , is given by Yamaguchi and can be applied in all overlap limits. The expressions above are widely employed on organic diradicals and dinuclear inorganic complexes with one or more electrons per magnetic site.^{1,17} On the other hand, in systems with multiple magnetic sites, such as in single molecule magnets, there are several exchange interactions. For such systems, spin topology can become a reliable alternative to predict their magnetic status, albeit in a qualitative way.¹⁸ In one of our recent works, the ground state spin density distribution has been utilized to estimate the exchange coupling constant in systems with multiple magnetic sites.¹⁹ The importance of spin topology in explaining the magnetic behavior had been highlighted by McConnell early in 1963.²⁰ On the basis of the HDVV Hamiltonian, he proposed the following spin density representation of exchange interaction:

$$\hat{H} = -\hat{S}^{\text{A}} \cdot \hat{S}^{\text{B}} \sum_{ij} J_{ij}^{\text{AB}} \rho_i^{\text{A}} \rho_j^{\text{B}} \quad (3)$$

This Hamiltonian elucidates the exchange interaction between two aromatic radical fragments A and B, where \hat{S}^{A} and \hat{S}^{B} are the total spin operators for A and B; ρ_i^{A} and ρ_j^{B} are the π -spin densities on atoms i and j of fragments A and B, respectively. In this expression, the exchange integral, which is evaluated in the context of valence bond theory,²¹ is usually considered as negative. As a consequence, ferromagnetic exchange interaction is found to be associated with the negative value of the spin density product.²² This model to predict the nature of magnetic interaction based on spin density has been popularly known as the McConnell-I model. In an effort to find out the effect of nonorthogonality in the broken symmetry approach, Caballol et al. expressed the coupling constant J , which takes

the following expression with the same form of HDVV Hamiltonian as used for eq 2:

$$J = \frac{(E_{\text{BS}} - E_{\text{T}'})}{1 + S_{\text{ab}}^2} \quad (4)$$

where E_{BS} and $E_{\text{T}'}$ are the energies of the unrestricted BS and triplet state and S_{ab} is the overlap integral between the magnetic orbitals of the broken symmetry solution.²³ They could find that the overlap term in the denominator of eq 4 is related to the spin density of magnetic center, ρ_{A} , as

$$S_{\text{ab}}^2 = 1 - \rho_{\text{A}}^2 \quad (5)$$

This relation is further modified by Boiteaux and Mouesca as

$$S_{\text{ab}}^2 = \rho_{\text{HS}}^2(\text{Cu}) - \rho_{\text{BS}}^2(\text{Cu}) \quad (6)$$

and used to quantify the antiferromagnetic (AFM) contribution to the exchange coupling between metal spins in ligand-bridged Cu(II) dimers.²⁴ Ruiz et al. suggested that this difference of spin densities at metal atoms in the high spin and BS state can be a good alternative to the direct calculation of overlap integral.²⁵ All of these facts suggest a link between the exchange coupling constant and spin density and hence validate a spin topology based interpretation of the magnetic nature. In fact, the McConnell-I model has long been used in designing high-spin organic ferromagnets.²⁶ In the inorganic regime also, a comprehension of spin density distribution is foreseen as a useful tool for designing FM or AFM interaction between paramagnetic centers in systems with multiple magnetic sites.^{19,27} Besides intramolecular magnetic interaction, the nature of intermolecular spin exchange has also been predicted from the polarized spin density of separate molecular units.^{22,28}

The foregoing discussion highlights the importance of spin topology in predicting the magnetic nature of a system. However, in the state-of-the-art formalisms (eqs 2, 4), any kind of such a direct correspondence between the coupling constant and spin density is absent. Although, in a few of the earlier works, it has been shown that the exchange coupling constant is related to the spin density; the relation has not widely been adopted for estimation of J . The oldest model in this concern is the McConnell-I model. Its validity has been confirmed through the ESR data obtained for [2.2] paracyclophane isomers.²⁹ This analogy with experimental observation as well as the agreement with the results of ab initio computations on model systems has made the McConnell-I model a reliable tool in predicting magnetic nature.³⁰ In spite of this, the McConnell-I model is questioned for its "ad hoc" way of proposition based on eq 1.³¹ Novoa and co-workers enquired about the validity of eq 3 by comparing it with the Heisenberg Hamiltonian and could find a direct correspondence between the spin density product and two electron exchange density matrix elements.^{31a} However, they stated this correspondence to be partly accidental. In an alternative model, the equality in eq 6 correlates the coupling constant with spin density. However, this model applies only to symmetric binuclear complexes with one unpaired electron per paramagnetic center.²⁵ All of these aspects invoke serious doubt for the general applicability of existing spin density based models and call upon the necessity of this work.

In the present work, an effort is made to correlate the spin topology with the exchange coupling constant in the case of two different types of exchange mechanisms, viz., direct exchange and superexchange. To quantify direct exchange,

the exchange part of a general many body Hamiltonian is modified in terms of spin density to set the required correlation. Whereas, in dealing with the superexchange mechanism, Anderson's pioneering work appears to be a good starting point.³² In this model, Anderson described the system to be perturbed by the intersite electron transfer and expressed the exchange energy in terms of second order perturbation energy. Here, we recast this expression with spin density. Such obtained spin density representations of the exchange interactions are applied on few previously studied magnetic systems to estimate the exchange coupling constants therein. The formalism for direct exchange is first verified with simple neutral and cationic Cr and Mn dimers followed by three large organic diradicals. The magnetic nature of Cr and Mn dimers has already been the subject of several theoretical and experimental investigations.³³ Desmaris et al. suggested a change in the magnetic nature of Cr₂ upon ionization, whereas the ferromagnetic ground state is reported for Mn₂ in its neutral as well as its cationic state.^{33a} The MRCI techniques predict the singlet ground state of Mn₂, whereas a number of DFT based computations conclude an 11-tuplet state as the ground state.^{33b} This elusive nature of Mn₂ has long been the subject of debate and was addressed in one of our previous works.^{33c} A recent synthesis of a ferromagnetic ultrathin Mn nanosheet by Mitra et al. solicits for its high spin ground state.^{33d} Among the organic diradicals chosen, widely cultivated 1,1',5,5'-tetramethyl-6,6'-dioxo-3,3'-biverdazyl (bisoxoverdazyl) is selected from the popular open shell database of representative systems, used by Valero et al.¹³ and later on Rivero et al.^{14a} to judge the performance of M06 and range separated functionals in an accurate estimation of *J*. The biverdazyl diradical consists of one unpaired electron on the π system of each ring, which all couple antiferromagnetically.^{13,14a,17a} Such organic radicals, when coupled through azobenzene, exhibit a photoinduced change in magnetism and constitute an interesting class of materials.^{17b} This spin crossover is attributed to the change in the conformation of these systems from trans to cis around the double bond. A loss of planarity in the cis form makes the intervening exchange path unavailable for the spins and the radical sites execute through space direct exchange. Here, two such cis azobenzenes, one linked with nitronyl nitroxide (azobenzene-nno) and the other with a verdazyl radical (azobenzene-ver), are also included as model systems. On the other hand, to deal with superexchange, anionic oxides of Cr and Mn are selected from one of our previous works, where they appeared as ferromagnets.^{33c,34} Apart from these, three other Cu binuclear complexes are selected from the open shell database,¹³ which include Cu₂Cl₆²⁻, [Cu(phen)₂(μ -AcO)(μ -OH)](NO₃)₂·H₂O, and [Cu(bpy)(H₂O)(NO₃)₂](μ -C₂O₄). The first of this list, Cu₂Cl₆²⁻, exhibits antiferromagnetism in its planar configuration.^{13,23} In the second complex, referred to as YAFZOU in the database, the Cu(II) atoms are reported to be ferromagnetically coupled. The third candidate, BISDOW, is known to have an antiferromagnetic ground state. Since, in these systems, the exchange interaction is mediated through the diamagnetic bridging ligand, the total coupling constant in a superexchange process should have contributions from the metal–ligand and metal–metal interactions. Earlier studies pointed out two such contributions to the magnetic coupling: $J = J_F$ (for FM interaction) + J_{AF} (for AFM interaction) = $2K_{ab} - 4t_{ab}^2/U$, where K_{ab} describes the direct exchange between magnetic orbitals and is generally considered as a ferromagnetic contribution.³² The second part, including the hopping integral

t_{ab} and the on-site Coulomb repulsion U , is usually termed kinetic exchange in Anderson's interpretation and antiferromagnetically contributes to the total coupling constant.⁴ In their seminal works, Calzado et al. applied CI techniques to compute these individual contributions to the magnetic coupling constant using effective Hamiltonian theory.³⁵ They have shown that it is also possible to extract these three parameters, K_{ab} , t_{ab} and U , using different solutions of Kohn–Sham equations.^{35b} The present spin density based formalism also enables one to partition the total coupling constant in a superexchange process into the contributions from the metal–ligand and metal–metal interactions. However, the variant magnetic systems opted for use in numerical validation can be categorized into four classes. The first group contains simple transition metal dimers executing direct exchange with more than one electron per magnetic site. Three large organic diradicals with dispersed spin in the ring are also taken as test systems for direct exchange in the second category. As the exhibitors of superexchange, systems with a single atomic ligand-bridged metal dimer are taken to constitute the third group. The candidates in the fourth category also execute a superexchange mechanism, but the metals are linked via extended bridging ligands in this case. In each of these categories, both the ferromagnetic and antiferromagnetic representatives are addressed. Numerical analysis with such a wide spectrum of reference systems provides the opportunity to verify the general applicability of the present formalism.

THEORY

Direct Exchange. Let us consider a system of N atoms, localized on n lattice sites. In compliance with the unrestricted formalism, a separate set of orbitals with different space parts is assigned for up-spin and down-spin electrons. Here, a $\sum_{a=1}^{n_i}$ set of electronic orbitals in atom A at site i is considered to represent such unrestricted MOs, occupied by a particular type of spin, λ or λ' . Electronic interactions in such a system can be described by the Hamiltonian:

$$\hat{H} = \sum_{i,a} \frac{p_{n_i^a}^2}{2m} - \sum_{i,a} \frac{Z_i e^2}{|r_i^a - R_i|} + \sum_{i,j} \frac{e^2}{|r_i^a - r_j^b|} \quad (7)$$

a, b

Many electron wave functions representing the above system can be expanded in terms of the products of single particle wave functions, which in turn are the orthonormal spin–orbital components of a Slater determinant. This complete orthonormal set of spin orbitals can be expressed in terms of single particle Wannier function $\phi_{n_i^a}(r - r_i^a)$, which is used to expand the field operator $\psi_{i\lambda}$,^{32b,36}

$$\psi_{i\lambda} = \sum_{a} \phi_{n_i^a}(r - r_i^a) f_{n_i^a\lambda}(r_i^a) \quad (8)$$

where $f_{n_i^a\lambda}$ is the fermion annihilation operator which annihilates a λ spin in the orbital n_i^a . Using this second quantized form of the operator, the expectation value arising from the third term of the Hamiltonian in eq 7 describes the exchange interaction^{32,36}

$$E_{DX} = \sum_{i < j} \sum_{a,b} \sum_{\lambda, \lambda'} J_{n_i^a n_j^b} f_{n_j^b\lambda'}^\dagger(r_j^b) f_{n_i^a\lambda}^\dagger(r_i^a) f_{n_j^b\lambda}(r_j^b) f_{n_i^a\lambda'}(r_i^a) \quad (9)$$

where

$$J_{n_i^a n_j^b} = \left\langle \varphi_{n_j^b \lambda'}^*(r - r_j^b) \varphi_{n_i^a \lambda}^*(r - r_i^a) \left| \frac{e^2}{|r_i^a - r_j^b|} \right| \varphi_{n_j^b \lambda} \right. \\ \left. \times (r - r_j^b) \varphi_{n_i^a \lambda}(r - r_i^a) \right\rangle \quad (10)$$

Now, it is known that the direct exchange involves only the electrons in magnetic orbitals. Between the spatially different up-spin and down-spin unrestricted MOs, the MO which does not have any population in its counterpart is considered the magnetic orbital. However, the population status of the molecular orbitals (MOs) is not sufficient to determine their singly or doubly occupied nature. In order to determine the occupancy status of any orbital, one has to check whether there is any overlap between an up-spin orbital and its corresponding pair down-spin orbital.³⁷ A zero overlap between an occupied up-spin MO and its corresponding pair down-spin MO can ascertain the singly occupied nature of the up-spin MO. In the present treatment, a n_i^a or n_j^b set of unrestricted MOs is considered to have such a singly occupied nature, which only participates in the direct exchange mechanism. Assuming one specific type of spin for one magnetic site and applying the fermion anticommutation rule as follows:

$$\{f_{n_i^a \lambda}^\dagger, f_{n_j^b \lambda'}\} = \delta_{ij} \delta_{\lambda \lambda'} \quad (11)$$

eq 9 can be simplified to represent the direct exchange as

$$E_{DX} = - \sum_{i < j} J_{n_i^a n_j^b} f_{n_j^b \lambda'}^\dagger(r_j^b) f_{n_j^b \lambda'}(r_j^b) f_{n_i^a \lambda}^\dagger(r_i^a) f_{n_i^a \lambda}(r_i^a) \\ a, b \\ \lambda, \lambda' \quad (12)$$

Now, as the n_i^a state is singly occupied by λ spins only, the number operator $\hat{N}_{n_i^a \lambda}(r_i^a)$ can also be regarded as the spin density operator $\hat{\rho}(r_i^a)$, and thus

$$f_{n_i^a \lambda}^\dagger(r_i^a) f_{n_i^a \lambda}(r_i^a) = \hat{N}_{n_i^a \lambda}(r_i^a) = \hat{\rho}(r_i^a) \quad (13)$$

Hence, with this form of spin density operator, it becomes straightforward to express eq 12 in terms of spin density

$$E_{DX} = - \sum_{i < j} J_{n_i^a n_j^b} \rho(r_j^b) \rho(r_i^a) \\ a, b \quad (14)$$

Equation 14 delineates the dependence of direct exchange interaction on the spin density of magnetic sites. Although, this expression includes the effect of spin density in the Hamiltonian similar to the form proposed by McConnell in eq 3; this is obtained from HDVV Hamiltonian through a sequence which has been absent in the formulation of McConnell's spin density Hamiltonian.³¹

Superexchange. The extent of direct exchange between magnetic sites gradually weakens with the increase in their distance,^{33c} as can also be understood from the presence of the $e^2|r_i^a - r_j^b|^{-1}$ term in the exchange parameter (eq 10). However, the unpaired electrons in remote magnetic sites still

may interact via a diamagnetic bridging group, which is defined as superexchange.³² This necessitates a nonorthogonal condition among the valence MOs of magnetic sites and the intervening diamagnetic ligand. Kramers applied perturbation theory to obtain the effective exchange resulting from this mechanism.³⁸ Anderson reformulated Kramers' theory by including the ligand wave function which is the covalent admixture of cation and anion wave functions.^{32b} To parametrize superexchange with spin density, a model system A–X–B is taken, where A and B are remote magnetic centers, intervened by a diamagnetic bridging group X. The active MOs in A and B are taken to be the set of $\sum_{a=1} n_i^a$ and $\sum_{c=1} n_k^c$ orbitals, respectively, singly occupied by λ or λ' type spins (Figure 1). In compliance with the unrestricted formalism,

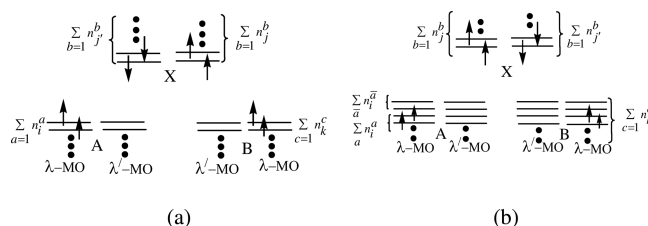


Figure 1. Representation of electronic arrangements in the model system A–X–B undergoing superexchange with (a) “both more than half full” and (b) “less than half full” d states as described by Anderson.

different sets of orbitals (for example, $\sum_{b=1} n_j^b$ and $\sum_{b=1} n_j^b$ in X) are assigned for λ and λ' types of spins.³⁷ Now, the magnetic orbitals in A or B may be fully or partially occupied, which is “both more than half full” and “less than half full” case.³² Since, in Anderson's model, an electron transits without spin flip,^{32b} a change in the occupancy status of MOs discriminates the nature of interaction. In the case of the full occupancy of λ orbitals on A or B, it becomes possible for λ' spin only to enter the set of λ' -MOs on A or B from $\sum_b n_j^b$ on X. The second order perturbation energy associated with such an electron transfer is expressed as^{32b}

$$\Delta E = \sum_{i', j'} \frac{t_{i' j'}^2}{U} \left(\frac{1}{2} + 2 \hat{S}_{n_i^a}(r_i^a) \cdot \hat{S}_{n_j^b}(r_j^b) \right) \\ a, b \quad (15)$$

where $t_{i' j'}$ is the hopping integral which carries an electron from X to A and U is the single ion repulsion energy. Now, the spin momentum operators can be split into different components as

$$\hat{S}_{n_i^a} \cdot \hat{S}_{n_j^b} = \hat{S}_{n_i^a}^x \cdot \hat{S}_{n_j^b}^x + \hat{S}_{n_i^a}^y \cdot \hat{S}_{n_j^b}^y + \hat{S}_{n_i^a}^z \cdot \hat{S}_{n_j^b}^z \quad (16)$$

Using the Jordan–Wigner transformation³⁹

$$S_{n_i^a}^+ = S_{n_i^a}^x + i S_{n_i^a}^y = f_{n_i^a}^\dagger \exp(i\pi \sum_{x < a} n_i^x) \text{ and} \\ S_{n_i^a}^- = S_{n_i^a}^x - i S_{n_i^a}^y = f_{n_i^a} \exp(-i\pi \sum_{x < a} n_i^x) \quad (17)$$

and following form of spin density operator⁴⁰

$$\hat{\rho}_{n_i^a} = 2 \hat{S}_{n_i^a}^z \delta(r - r_i^a) \quad (18)$$

where $\hat{\rho}_{n_i^a}$ is the spin density operator at the state n_i^a ; eq 16 can be written as

$$\hat{S}_{n_i^a} \cdot \hat{S}_{n_j^b} = \frac{1}{2} (f_{n_i^a}^\dagger f_{n_j^b} + f_{n_j^b}^\dagger f_{n_i^a}) + \frac{1}{4} \rho_{n_i^a} \cdot \rho_{n_j^b} \quad (19)$$

Applying the anticommutation rule in eq 11, the first term within the parentheses in eq 19 vanishes. Inserting this simplified form in eq 15, the interaction between A and X can be expressed as

$$\Delta E = \frac{1}{2} \sum_{i',j'} \frac{t_{r_{i'}^a r_{j'}^b}^2}{U} (1 + \rho_A(r_i) \cdot \rho_X(r_j)) \quad (20)$$

where ρ_A is the overall spin density at A. While this dispersal of λ' spins from $\sum_b n_j^b$ orbitals on X goes on, there operates a direct exchange among localized spins on A and B (Figure 1a), which is expressed through eq 14. Therefore, the total energy in a superexchange process for all of these magnetic interactions among A, X, and B can be written as

$$E_{SX} = \frac{1}{2} \sum_{i',j'} \frac{t_{r_{i'}^a r_{j'}^b}^2}{U} (1 + \rho_A(r_i) \cdot \rho_X(r_j)) - \sum_{i,k} J_{AB} \rho_A(r_i) \rho_B(r_k) \quad (21)$$

From this expression, a partitioning of the total coupling constant can be figured out. The first part accounts for the metal–ligand interaction, and the coupling between metal spins is addressed in the second part. In fact, the t^2/U term is related to J for metal–ligand interaction in the well-known Hubbard model Hamiltonian.^{6,23} The parameters t and U in the Hubbard Hamiltonian are obtained through a second quantization of the one electron and two electron operators in the many body Hamiltonian (eq 7) through the field operator in eq 8.³⁶ Hence, the integral form of the operators can be written as

$$t_{ij} = \int dr \varphi(r - r_i) \left(\frac{p^2}{2m} \right) \varphi(r - r_j) \text{ and} \\ U = \int dr_i \int dr_j |\varphi(r - r_i)|^2 \left(\frac{e^2}{r_i - r_j} \right) |\varphi(r - r_j)|^2 \quad (22)$$

Several works are devoted for the estimation of these parameters t and U .^{23,35} However, in the present work, instead of the direct estimation of t and U , eq 20 is used to extract the magnetic coupling constant (or t^2/U) from the second order perturbation energy for intersite charge transfer and the spin densities on the concerned sites. The second order energy corresponding to the charge transfer is computed using the natural bond orbital (NBO) analysis, which is discussed in detail for particular systems in the following section. On the other hand, J_{AB} in the second part of eq 21 estimates direct exchange. Hence, the total coupling constant (J_{SX}) in a superexchange process can be decomposed into the coupling of metal and ligand spins (J_{ML}) and that between metallic spins (J_{MM}), which may be expressed as follows:

$$J_{SX} = \sum_{i,j} \frac{2\Delta E}{1 + \rho_A(r_i) \cdot \rho_X(r_j)} - \sum_{i,k} \frac{E_{DX}}{\rho_A(r_i) \rho_B(r_k)} \equiv J_{ML} + J_{MM} \quad (23)$$

Such splitting of the coupling constant, which is very similar to the Anderson's interpretation,³² is exercised in several references.^{28,35,41} The FM interaction is considered to be comparatively weaker because it operates between spatially orthogonal wave functions.^{41c} However, ab initio results suggest that the sign of J_{MM} may also deviate from its usual positive sign and depends upon spin polarization of the system,^{35b} which is also apparent from eq 23. Moreover, the kinetic exchange may not be always negative and can have a ferromagnetic nature.^{41b} An explanation for this exception also may be inherent in the above expression since each interaction is governed by spin topology. In the whole mechanism, one can easily deduce the concomitant spin topology. The magnetic orbitals in A and B, i.e., the set of $\sum_a n_i^a$ and $\sum_c n_k^c$, are primarily assumed to be occupied by λ spins. So far as the spin density of diamagnetic X (ρ_X) is concerned, it is dependent on the ultimate difference of majority and minority spins during superexchange

$$\rho_X = \sum_{j,j'} (\rho_{n_j^b, \lambda'}(r_j^b) \sim \rho_{n_j^b, \lambda}(r_j^b)) \quad (24)$$

Depending upon the “both more than half full” or “less than half full” d states as described by Anderson, the nature of intersite charge transfer may vary, which in turn leads to a different spin topology of the system. In the case where the λ -spin orbitals in A and B are “more than half full”, the λ' spins get dispersed from the $\sum_b n_j^b$ orbitals, whereas λ spins on $\sum_b n_j^b$ remain localized on X. Thus, there occurs excess accumulation of λ spins (eq 24). Consequently, an identical λ spin density is expected on each of the A, X, and B atoms.

A similar treatment for “less than half full” states, where few of the states (say, $\sum_{\bar{a}} n_i^{\bar{a}}$ on A) remain completely empty, had also been proposed by Anderson.^{32b} In this situation, the transfer of an electron together with an additional internal exchange effect induces a third-order perturbation to the system. Let us consider that the transition is taking place from the $\sum_b n_j^b$ orbital on X to one of the empty states $\sum_{\bar{a}} n_i^{\bar{a}}$ on atom A, where another set of orbitals $\sum_a n_i^a$ is singly occupied by λ spins (Figure 1b). With this assumption, the third order interaction is expressed as

$$\Delta E' = \sum_{i,j} \frac{t_{r_j^b r_i^{\bar{a}}}^2 J_{n_i^a n_i^{\bar{a}}}}{U^2} f_{n_i^a, \lambda}^\dagger(r_i^a) f_{n_j^b, \lambda'}^\dagger(r_j^b) f_{n_i^a, \lambda}(r_i^a) f_{n_j^b, \lambda}(r_j^b) \quad (25)$$

a, \bar{a}, b
 λ, λ'

Now, since the spin transfers without flipping, the presence of λ spins in the $\sum_a n_i^a$ set of orbitals allows the λ spins only to enter the empty $\sum_{\bar{a}} n_i^{\bar{a}}$ states obeying Hund's rule of maximum spin multiplicity. In this condition, where all of the spins are λ , the above expression with application of the fermion anticommutation rule (eq 11) and spin density operator (eq 13), transforms as follows:

$$\Delta E' = - \sum_{i,j} \frac{t_{r_j^b r_i^{\bar{a}}}^2 J_{n_i^a n_i^{\bar{a}}}}{U^2} \rho(r_i^a) \rho(r_j^b) \quad (26)$$

a, \bar{a}, b, λ

However, this third order correction term becomes insignificant for a large antiferromagnetic interaction between the cation and

ligand.^{32b} Beside λ spins, there also exists the possibility of λ' spin hopping from $\sum_i n_i^b$ on X to unoccupied λ' spin orbitals of atoms A and B at sites i and k . However, existing λ spin moments in A or B facilitate λ spin hopping onto their empty orbital. Therefore, more delocalization of λ spins from X compared to λ' spins should effect an overriding population of λ' spin on X (eq 24). Hence, the overall spin topology should display an opposite spin density on X to that on both of the A and B atoms.

NUMERICAL VERIFICATION

To verify the reliability of the present formalism, a broad class of systems with a known magnetic status, as mentioned earlier in the Introduction, is selected. Magnetic characterization of such systems is performed within the framework of density functional theory. DFT is known to produce an accurate spin density value which is also the key parameter in the present work.⁴² Throughout this study, we stick to the B3LYP exchange-correlation functional in an unrestricted framework. Geometries of simple systems such as transition metal dimers and their anionic oxides are optimized with the 6-311+g (3df) basis set using GAUSSIAN03W.⁴³ The coordinates of cis azobenzene-nno and azobenzene-ver, optimized with the 6-311+g(d,p) basis set, are collected from ref 17b. The rest of the systems, viz. bisoxoverdazyl, $\text{Cu}_2\text{Cl}_6^{2-}$, YAFZOU, and BISDOW, are included in the open shell database, and their ground state geometries are taken from various sources mentioned therein.^{13,44} Such obtained coordinates of the systems in their ground states are used in ORCA to perform broken symmetry calculations.⁴⁵ Though accurate wave function methods could readily be applied on simple systems, for a uniform comparison, the DFT-based methods are maintained throughout this work. The broken symmetry solution is obtained from an initial guess generated by flipping the local spin density in either of the magnetic centers of the high spin solution.^{45,46} This technique, known as the spin flip DFT (SF-DFT), is employed to compute the high-spin-BS energy gap. This is comparable with another approach SF-TDDFT adopted by Krylov and co-workers.⁴⁷ In this method, starting from a reference high spin state, both the closed shell singlet and $M_s = 0$ state of a triplet can be generated and used to estimate high-spin–low-spin energy splitting.⁴⁸ This formulation, based on the noncollinear XC potential, can deal with the spin flip transition in addition to the transition treated in ordinary TDDFT. With a proper DFT formalism, this method is found to be efficient in correctly describing the multiplicity changing excitations.⁴⁹ Moreover, the comparison of coupling constants through this SF-TDDFT and conventional broken symmetry approach concludes that, in DFT calculations, the spin symmetry must be considered through the spin projected methods.⁵⁰ However, the energy difference of high spin and BS spin states, evaluated through the SF-DFT method, is mapped onto E_{DX} in eq 14, and this enables a straightforward determination of the exchange-coupling constant (J_{DX}) as follows:

$$J_{\text{DX}} = -\frac{E_{\text{HS}} - E_{\text{BS}}}{\rho_{\text{A}}\rho_{\text{B}}} \quad (27)$$

The spin densities on magnetic sites (A and B) in the denominator are obtained from the Mulliken population of the high spin state, which is taken as the reference state in the SF-DFT approach. The exchange-coupling constants (J_{DX}) of tran-

sition metal dimers, obtained through eq 27, are found to be concordant with the coupling constant values (J_{Y}) employing the approximate spin projection technique of Yamaguchi (Table 1).

Table 1. Comparison of Coupling Constants (J_{DX}) Obtained through eq 27 and Approximate Spin Projection Technique of Yamaguchi (J_{Y}) for Cr_2 , Mn_2 , and Their Cations^a

| systems | ρ_{M1} | ρ_{M2} | $E_{\text{HS}} - E_{\text{BS}}$ (cm^{-1}) | J_{DX} (cm^{-1}) | J_{Y} (cm^{-1}) |
|-----------------|--------------------|--------------------|--|--------------------------------------|-------------------------------------|
| Cr_2 | 5 | 5 | 3408.620 | −136.34 | −137.38 |
| Cr_2^+ | 5.5 | 5.5 | −98490.635 | 3255.89 | 3181.09 |
| Mn_2 | 5 | 5 | −11489.881 | 459.60 | 441.82 |
| Mn_2^+ | 5.5 | 5.5 | −7433.394 | 245.73 | 241.08 |

^aSpin densities on first and second metals are denoted as ρ_{M1} and ρ_{M2} .

Unlike these transition metal systems, where huge spin is localized on the metal centers, in organic diradicals (Figure 2),

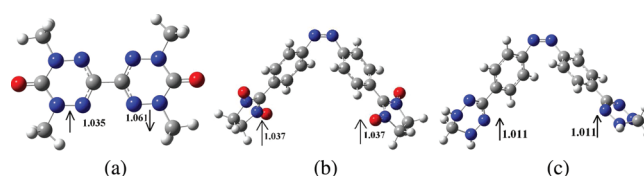


Figure 2. Ground state spin topology in (a) bisoxoverdazyl, (b) azobenzene-nno, and (c) azobenzene-ver (up-arrow, down-arrow, and corresponding numerical values signify up- and down-spin densities, respectively).

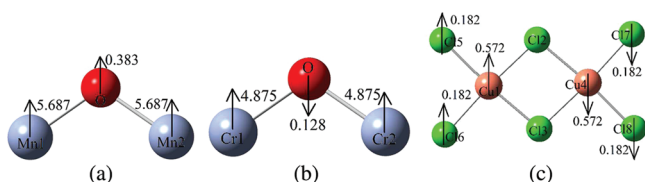
spins are distributed throughout the network. Thus, to apply eq 27 on these systems, dispersed spins are summed up to get the overall spin density in the left and right wings of the molecules. A 6-311+g(d,p) computation on such systems produces the overall spin density in the left wing (ρ_{L}) and right wing (ρ_{R}) as follows. Similar to Table 1, the coupling constants (J_{DX}) of the above three systems are in proximity to the J_{Y} (Table 2).

Now, turning to superexchange, three systems with the metals coupled via a single atomic ligand are primarily selected. Among these, anionic oxide clusters of Cr and Mn have already been reported as ferromagnets in one of our previous works.^{33c,34} Another simple yet widely cultivated system, $\text{Cu}_2\text{Cl}_6^{2-}$, is taken from the open shell database of Truhlar and co-workers.^{13,23,35} The different spin topologies in these systems (Figure 3) are intriguing and demand evaluation in light of the present formalism. Optimization of these two clusters at the UB3LYP/6-311+g(3df) level of computation produces similar spin density to the previous results. Between these two, the spin distribution in Mn_2O^- (Figure 3a) represents “both more than half full” occupancy status of the d states to and from which the transition is taking place.^{32b} In this situation, A, X, and B are proposed to have identical spins on them, which is in complete agreement with the computed spin topology of Mn_2O^- (Figure 3a). On the other hand, in Cr_2O^- , the spin density values (Figure 3b) resembles the “less than half full” case described by Anderson.³² The spin topology (Figure 3b) in this case again matches with proposed alternation of spin density. Next, we put our effort to quantify the exchange interaction in these molecules executing superexchange. Since all of the elements in Mn_2O^- exhibit an identical spin density, a ferromagnetic exchange among these polarized spins is expected. Computation of the exchange coupling constant through the spin projection technique of Yamaguchi comes out with a positive value of J_{Y} and stands for spin topology based prediction.

Table 2. Comparison of Coupling Constants Obtained through eq 27 (J_{DX}), Approximate Spin Projection Technique of Yamaguchi (J_{Y}), and Experiment (J_{expt})¹³ for the Systems in Figure 2^a

| systems | ρ_{l} | ρ_{r} | $E_{\text{HS}} - E_{\text{BS}}$ (cm^{-1}) | J_{DX} (cm^{-1}) | J_{Y} (cm^{-1}) | J_{expt} (cm^{-1}) |
|----------------|-------------------|-------------------|--|--------------------------------------|-------------------------------------|--|
| bisoxoverdazyl | 1.035 | 1.061 | −666.333 | −606.64 | −650.38 | −769 |
| azobenzene-nno | 1.037 | 1.037 | 63.648 | 59.24 | 62 | |
| azobenzene-ver | 1.011 | 1.011 | 79.010 | 77.28 | 79 | |

^aSpin densities on the left and right wings of the diradicals are denoted as ρ_{l} and ρ_{r} .

**Figure 3.** Ground state spin topology in (a) Mn_2O^- , (b) Cr_2O^- , and (c) $\text{Cu}_2\text{Cl}_6^{2-}$ (up-arrow, down-arrow, and corresponding numerical values signify up- and down-spin densities respectively).

However, this coupling constant (J_{Y}) due to superexchange can be partitioned into the contribution from metal–metal (J_{MM}) and metal–ligand (J_{ML}) exchange, as suggested in eq 23. In order to quantify these contributions separately, we follow a recent computational scheme of our own.¹⁹ In this scheme, the ligand in the system is made a dummy, which means that, in the present case, O^{2-} remains there in the structure without any electronic contribution. This manipulation enables one to evaluate the intermetallic coupling constant ($J_{\text{Y}(\text{Mn-Mn})}$) only. A lower positive value of $J_{\text{Y}(\text{Mn-Mn})}$ than J_{Y} indicates that there exists a ferromagnetic exchange among the residual spins on the metal and ligand. Now, by subtracting $J_{\text{Y}(\text{Mn-Mn})}$ from J_{Y} , it becomes possible to get $2J_{\text{Y}(\text{Mn-O})}$, which defines the exchange interaction between Mn1-O and Mn2-O pairs. Again, the interaction between a particular pair of metal and ligand ($J_{\text{Mn-O}}$) is quantified through eq 20, and the result is multiplied by 2 for comparison with $2J_{\text{Y}(\text{Mn-O})}$. The second order perturbation energies (ΔE in eq 20) due to the charge transfer from O^{2-} to Mn1 and Mn2 are obtained from the natural bond orbital (NBO) output, carried out in Gaussian NBO, version 3.1.⁵¹ Within a series of ΔE values corresponding to charge transfer between several donors and acceptors, we have opted for a particular donor–acceptor pair which fits best to our present model. For example, in the “both more than half full” case, i.e., in Mn_2O^- , ΔE resulting from the transition of a down-spin from the lone pair of oxygen to the metal d orbital is used in eq 20. The orbital which has sp^2 character and contains a lone pair of electrons of oxygen is considered as the donor orbital. Whereas, the singly occupied metal orbital having significant d character is considered as the recipient of the charge. The analogy between coupling constant values estimated through two different approaches is reflected in Table 3.

A similar treatment is adopted for Cr_2O^- (“less than half full”) where the ΔE corresponding to the up-spin transfer from the ligand to metal is considered. In Cr_2O^- , the spin topology suggests a ferromagnetic coupling among the parallel spins on Cr atoms, and antiparallel spin alignment in Cr and O leads to an antiferromagnetic interaction (Figure 3b). This becomes evident from the large negative value of coupling constant ($J_{\text{Y}(\text{Cr-O})}$) obtained by the spin projection technique (Table 3). Again, eq 20 is employed to find $J_{\text{Cr-O}}$, which agrees well with the $J_{\text{Y}(\text{Cr-O})}$ value (Table 3) and hence validates eq 20.

In the third reference system $\text{Cu}_2\text{Cl}_6^{2-}$, along with the bridging chlorides, terminal ligands also show significant spin density, which might have a role in the spin exchange. For comparison with ab initio results, all of the bond lengths and angles of $\text{Cu}_2\text{Cl}_6^{2-}$ are kept the same as in ref 23. The Cu–Cu distance is made equal with the experimental value of 3.44 Å.^{35b} The planar configuration of this geometry is reported to have an antiferromagnetic nature,^{23,35} which is also confirmed from the antiparallel spin alignment on Cu atoms (Figure 3c). Cu(II) has all of the λ -MOs filled up, and hence down-spins from the bridging chlorides (Cl2 and Cl3) and terminal chlorides (Cl5 and Cl6) may disperse into the vacant λ' orbital on Cu1. Remaining λ spins on bridging chlorides induce λ' spin density on Cu4 through bonding interaction. Equal dispersal of λ and λ' spins from bridging chlorides onto Cu4 and Cu1, respectively, should leave no excess spin on bridging chlorides according to eq 24. This fact is attested from the zero spin density on the bridging chlorides (Figure 3c). Consistent with the available reports, this system produces a small negative value of exchange coupling constant (J_{Y}) upon application of the Yamaguchi formula (Table 4). With dummy bridging chlorides, a negligible AFM interaction is obtained between segregated left and right CuCl_2 units. Hence, the coupling constant value can be considered to originate solely from the Cu–Cl interactions. Again, the spin topology suggests that the interaction of metals and terminal chlorides ($J_{\text{Cu-Cl}}^{\text{t}}$) should differ from the coupling among metal and bridging chlorides ($J_{\text{Cu-Cl}}^{\text{b}}$). Identical spin densities on terminal ligands and allied metals indicate a positive value of $J_{\text{Cu-Cl}}^{\text{t}}$. On the other hand, a zero spin density on bridging chlorides makes it difficult to predict the nature of $J_{\text{Cu-Cl}}^{\text{b}}$. However, according to Anderson, the admixing of ligand and metal orbitals leads to an antiferromagnetic interaction among metals and bridging chlorides.^{32b} Now, to

Table 3. Comparison of the Metal–Ligand Contribution ($J_{\text{M-O}}$) Towards the Total Coupling Constant Obtained through eq 20 and the Approximate Spin Projection Technique of Yamaguchi ($J_{\text{Y}(\text{M-O})}$), Which in Turn Is Derived by Subtracting the Coupling Constant ($J_{\text{Y}(\text{M-M})}$) with Dummy Bridging Atom O^{2-} from the Total Coupling Constant (J_{Y}) through the Yamaguchi Expression^a

| systems | through spin-projection technique | | | employing eq 20 | | | |
|---------|-------------------------------------|---|--|-------------------|-------------------|-----------------------|--|
| | J_{Y} (cm^{-1}) | $J_{\text{Y}(\text{M-M})}$ (cm^{-1}) | $2J_{\text{Y}(\text{M-O})}$ (cm^{-1}) | ρ_{M} | ρ_{O} | ΔE (kcal/mol) | $2J_{\text{M-O}}$ (cm^{-1}) |
| M = Mn | 975.51 | 247.28 | 728.23 | 5.687 | 0.383 | 1.75 | 769 |
| M = Cr | 370.55 | 4619.55 | −4248.45 | 4.875 | 0.128 | 5.56 | −4789 |

^aM implies Mn and Cr for Mn_2O^- and Cr_2O^- , respectively. Spin densities on the metal and ligand are denoted as ρ_{M} and ρ_{O} .

Table 4. Comparison of Coupling Constants ($J_{\text{Cu-Cl}}$) Obtained through eq 28, Approximate Spin Projection Technique of Yamaguchi ($J_Y(\text{Cu-Cl})$) and Experiment (J_{expt})^{35a,b} for $\text{Cu}_2\text{Cl}_6^{2-}$

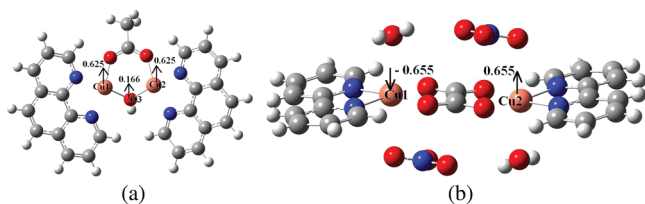
| $2\Delta E$ for Cu-Cl ^b pair (kcal/mol) | $2\Delta E$ for Cu-Cl ^t pair (kcal/mol) | $4J_{\text{Cu-Cl}}^b$ (kcal/mol) | $4J_{\text{Cu-Cl}}^t$ (kcal/mol) | $J_{\text{Cu-Cl}}$ (cm ⁻¹) | $J_Y(\text{Cu-Cl})$ (cm ⁻¹) | J_{expt} (cm ⁻¹) |
|--|--|----------------------------------|----------------------------------|--|---|---------------------------------------|
| 0.52 | 0.50 | -2.08 | 2.00 | -27.98 | -27.89 | -40 |

employ eq 20 in this system, second order perturbation energy (ΔE) corresponding to λ and λ' spin transfer from attached chlorides to Cu4 and Cu1 is taken into consideration. Ignoring small fractional values of spin density on both the metal and ligand, the first part of eq 23 takes the following form:

$$J_{\text{SX}} \approx 2\Delta E \quad (28)$$

Putting appropriate values of ΔE on this expression and summing up the positive and negative contribution from $J_{\text{Cu-Cl}}^t$ and $J_{\text{Cu-Cl}}^b$, respectively, total metal–ligand interaction ($J_{\text{Cu-Cl}}$) can be quantified, which is almost the same with J_Y (Table 4). Besides this analogy, the value of the coupling constant obtained through eq 28 is also found to be in parity with that evaluated through CI techniques and the experimental value (J_{expt}) as well (Table 4).^{35a,b} Again, quantification of the hopping integral t and on-site repulsion energy U through CASCI techniques yields $t^2/U = -4 \text{ cm}^{-1}$ for the system $\text{Cu}_2\text{Cl}_6^{2-}$.^{35a} This t^2/U term is considered to be equivalent to the coupling constant between each pair of metal and ligand in the framework of the Hubbard Hamiltonian.^{6,23} Since there are eight such pairs of metal and ligand in $\text{Cu}_2\text{Cl}_6^{2-}$, the total metal–ligand interaction is estimated as -32 cm^{-1} , which is close to the $J_{\text{Cu-Cl}}$ resulting from eq 28 (Table 4).

In the next category, two Cu dinuclear systems, having an extended bridging ligand between metals, are taken to apply upon the formalism. Among these candidates from the open shell database,¹³ in the ferromagnetic YAFZOU, Cu(II) spins are coupled through the bridging hydroxo and carboxylato ligands. Whereas in the second complex, BISDOW, the exchange interaction between Cu(II) cations is mediated by an oxalato bis-chelating anion. The frozen-core LANL2DZ basis set, an efficient performer particularly for metal systems,^{27c} is applied on these large systems to get their ground state spin topology (Figure 4) and coupling constant.

**Figure 4.** Ground state spin topology in (a) YAFZOU and (b) BISDOW (up-arrow, down-arrow, and corresponding numerical values signify up- and down-spin densities, respectively).

Since, in these systems, the metals are linked via extended ligands like carboxylato or oxalato, the analysis of NBO output to find out relevant charge transfers between the atoms becomes complicated. Regarding this, partitioning the molecule into fragments in which the charge transfer is taking place might be taken into consideration. Rudra et al. performed this kind of fragmentation for these systems, where the spin is not localized on a single atom.⁵² From the NBO output of the YAFZOU, the molecule is found to be fragmented into Cu1, Cu2, $\mu\text{-OH}$, and $\mu\text{-carboxylato}$. Occupied up-spin orbitals in

Cu(II) necessitate the migration of down-spin from the bridging ligands onto it. This fact is well supported by the presence of excess up-spin density on $\mu\text{-OH}$, following eq 24. Now, application of the Yamaguchi expression on the whole molecule gives the total coupling constant value (J_Y), while the same method results in a very weak coupling constant in YAFZOU with dummy bridging ligands. This signifies the absence of any through space interaction between metal spins making the J_{MM} term of eq 23 equal to zero. Thus, the total coupling constant is solely due to the metal–ligand interaction (J_{ML} in eq 23). From the NBO output, the vacant orbitals having dominant d orbital contribution are regarded as the acceptor orbitals in Cu(II), whereas nearly sp^3 hybridized orbitals containing the lone pair of oxygen are recognized as the donor orbitals on $\mu\text{-OH}$. In the case of the carboxylato ligand, any such relevant pair of donor–acceptor orbitals is found missing, and thus the superexchange is considered to be mediated only by $\mu\text{-OH}$. For negligible spin density product on the participating fragments, eq 28 applies to this system. This equation uses second order perturbation energies [ΔE ($\mu\text{-ligand} \rightarrow \text{Cu1}$) and ΔE ($\mu\text{-ligand} \rightarrow \text{Cu2}$)] for down-spin transfer from $\mu\text{-OH}$ to Cu1 and Cu2 to give the total coupling constant (J_{SX}), which appears to be in good agreement with J_Y (Table 5).

Table 5. Comparison of Coupling Constants (J_{SX}) Obtained through Present Formalism (eqs 28 and 20 for YAFZOU and BISDOW with Negligible and Significant Spin Density Product, Respectively), the Approximate Spin Projection Technique of Yamaguchi (J_Y), and Experiment (J_{expt})¹³

| systems | $2\Delta E$ ($\mu\text{-ligand} \rightarrow \text{Cu1}$) (kcal/mol) | $2\Delta E$ ($\mu\text{-ligand} \rightarrow \text{Cu2}$) (kcal/mol) | J_{SX} (cm ⁻¹) | J_Y (cm ⁻¹) | J_{expt} (cm ⁻¹) |
|---------|---|---|-------------------------------------|---------------------------|---------------------------------------|
| YAFZOU | 0.10 | 0.06 | 56 | 62 | 111 |
| BISDOW | 1.67 | 0.30 | -482 | -472 | -382 |

Unlike YAFZOU, there is no significant spin density on the bridging oxalato in BISDOW (Figure 4b). This fact, as also observed in $\text{Cu}_2\text{Cl}_6^{2-}$, can similarly be attributed to the equal dispersal of up-spin and down-spin from oxalato to Cu1 and Cu2. During the up-spin transfer, the molecule is partitioned into two fragments; one contains only Cu1, while Cu2 along with oxalate belongs to the other. On the other hand, the down-spin transfers to Cu2 from the fragment holding Cu1 and oxalate together. In both cases, the concerned fragments have a significant spin density of 0.655 and are antiparallel to each other and considered input in eq 20. To get the second order perturbation energy of this expression, nearly sp^2 orbitals of oxygen atoms in the bridging ligand are regarded as the gateways of spin transfer. Such an obtained coupling constant (J_{SX}) is regarded as the total coupling constant since application of the Yamaguchi expression on the system with dummy oxalato results in a very weak interaction, suggesting almost nil contribution from direct exchange (J_{MM} in eq 23). The sign and magnitude of the total coupling constant through the Yamaguchi technique (J_Y) agrees well with J_{SX} (Table 5).

CONCLUSION

In the present study, spin density emerges as an effective parameter in interpretation and quantification of the magnetic interaction. This work formulates the coupling constant in direct exchange and superexchange mechanisms through which the spins are coupled in most of the magnetic systems. The exchange part of a general Hamiltonian is operated on a multi-electronic state to describe the direct exchange interaction in terms of spin density, and thus the wave function concept is bridged with DFT. To deal with the superexchange process, the perturbative approach of Anderson is adopted. The total coupling constant in a superexchange mechanism is split into the contributions from metal–metal and metal–ligand interaction. The present formalism is employed on a wide spectrum of molecular systems which entail both the ferro- and anti-ferromagnetic compounds from the organic and inorganic domain. Among these, four systems, viz., bisoxoverdazyl, $\text{Cu}_2\text{Cl}_6^{2-}$, YAFZOU, and BISDOW, have confronted several ab initio and DFT studies.^{13,14,23,35a,b,50a,52} Comparisons of the reported coupling constant values in these references are found to be concordant with the J , resulting through present theory and hence solicits for the present theoretical construction. Moreover, the results are in good agreement with the values obtained through the well-known spin projection technique of Yamaguchi. The ground state spin topologies of these systems are also in parity with the sign of the coupling constant. In the systems, executing superexchange, the difference of spin topology is found to stem from the occupation status of the d states on the metals, to and from which the electron transfer takes place. The extent of overlap between the metal and ligand also governs the spin topology. In the case of the anionic oxide of Cr with “less than half full” d states, it is interesting to note an alternation of spin density in the spin topology of Cr_2O^- . The explanation given in this regard may also be useful to account for the well-observed spin density alternation in π -conjugated organic diradicals.^{17a–c,53}

In the estimation of the exchange coupling constant, DFT has to encounter two major difficulties. In the unrestricted Kohn–Sham method, $\langle S^2 \rangle$ is not well-defined, particularly in the broken symmetry state.^{1,15,50a,52} Valero et al. concluded that this spin square term should not always be used as a reliable indicator of the success of a given calculation.^{50a} Nevertheless, the present formalism offers a solution to this problem by using the spin density of the magnetic sites in estimation of J rather than the $\langle S^2 \rangle$ value of the spin configurations. The second bottleneck in using DFT lies in the choice of the proper combination of exchange–correlation functional and basis set for an accurate estimation of J .^{11,14a,c,52,54} However, the present work relates the exchange–coupling constant with spin density, which can be obtained both theoretically and experimentally.⁵⁵ Hence, one may explore the level of theory, which reproduces the experimentally obtained spin topology. Next, estimation of the other parameters in eq 23 at the same computational level may lead to a reliable value of the coupling constant. Thus, the present work may help in the proper selection of theoretical level for accurate estimation of J . Among the parameters in eq 23, spin density is a term which can be realized experimentally. In case the other parameters are obtained experimentally, this work is expected to guide the estimation of the coupling constant solely from experimental data. The recasting of the HDVV Hamiltonian in terms of spin density results in an expression similar to the well-known spin density Hamiltonian

proposed by McConnell, which has been the pioneer in spin-topology-based prediction of magnetic behavior. However, the way it was modeled on the basis of the HDVV Hamiltonian required a validation, which has been provided through the present formalism.

ASSOCIATED CONTENT

Supporting Information

Coordinates of all systems used for numerical verification are given in Tables S1–S12. This information is available free of charge via the Internet at <http://pubs.acs.org/>.

AUTHOR INFORMATION

Corresponding Author

*E-mail: anirbanmisra@yahoo.com.

Notes

The authors declare no competing financial interest.

ACKNOWLEDGMENTS

The authors thank the Department of Science and Technology, India for financial support.

REFERENCES

- (1) de P. R. Moreira, I.; Illas, F. *Phys. Chem. Chem. Phys.* **2006**, *8*, 1645–1659.
- (2) de P. R. Moreira, I.; Illas, F. *Phys. Rev. B* **1997**, *55*, 4129–4137.
- (3) de P. R. Moreira, I.; Illas, F.; Calzado, C. J.; Sanz, J. F.; Malrieu, J. P.; Amor, N. B.; Maynau, D. *Phys. Rev. B* **1999**, *59*, R6593–R6596.
- (4) Calzado, C. J.; Celestino, A.; Caballol, R.; Malrieu, J. P. *Theor. Chem. Acc.* **2010**, *126*, 185–196.
- (5) (a) Miralles, J.; Daudey, J. P.; Caballol, R. *Chem. Phys. Lett.* **1992**, *198*, 555–562. (b) Miralles, J.; Castell, O.; Caballol, R.; Malrieu, J. P. *Chem. Phys.* **1993**, *172*, 33–43.
- (6) Munoz, D.; Illas, F.; de P. R. Moreira, I. *Phys. Rev. Lett.* **2000**, *84*, 1579–1582.
- (7) (a) Andersson, K.; Malmqvist, P.-Å.; Roos, B. O.; Sadlej, A. J.; Wolinski, K. *J. Phys. Chem.* **1990**, *94*, 5483–5488. (b) Andersson, K.; Malmqvist, P.-Å.; Roos, B. O. *J. Chem. Phys.* **1992**, *96*, 1218–1226. (c) de Graaf, C.; Sousa, C.; de P. R. Moreira, I.; Illas, F. *J. Phys. Chem. A* **2001**, *105*, 11371–11378.
- (8) Guennic, B. L.; Robert, V. C. R. *Chim.* **2008**, *11*, 650–664.
- (9) (a) Noodleman, L. *J. Chem. Phys.* **1981**, *74*, 5737–5743. (b) Noodleman, L.; Case, D. A. *Adv. Inorg. Chem.* **1992**, *38*, 423–468.
- (10) (a) Becke, A. D. *J. Chem. Phys.* **1993**, *98*, 5648–5652. (b) Ernzerhof, M.; Scuseria, G. E. *J. Chem. Phys.* **1999**, *110*, 5029–5035.
- (11) de P. R. Moreira, I.; Illas, F.; Martin, R. L. *Phys. Rev. B* **2002**, *65*, 155102–155115.
- (12) (a) Zhao, Y.; Truhlar, D. G. *J. Chem. Phys.* **2006**, *125*, 194101–194118. (b) Zhao, Y.; Truhlar, D. G. *J. Phys. Chem. A* **2006**, *110*, 13126–13130.
- (13) Valero, R.; Costa, R.; de P. R. Moreira, I.; Truhlar, D. G.; Illas, F. *J. Chem. Phys.* **2008**, *128*, 114103–114110.
- (14) (a) Rivero, P.; de P. R. Moreira, I.; Illas, F.; Scuseria, G. E. *J. Chem. Phys.* **2008**, *129*, 184110–184116. (b) Peralta, J. I.; Melo, J. I. *J. Chem. Theory Comput.* **2010**, *6*, 1894–1899. (c) Phillips, J. J.; Peralta, J. E. *J. Chem. Phys.* **2011**, *134*, 034108–034114.
- (15) Md. Ali, E.; Datta, S. N. *J. Phys. Chem. A* **2006**, *110*, 2776–2784 and references therein.
- (16) (a) Ginsberg, A. P. *J. Am. Chem. Soc.* **1980**, *102*, 111–117. (b) Noodleman, L.; Davidson, E. R. *Chem. Phys.* **1985**, *109*, 131–143. (c) Bencini, A.; Gatteschi, D. *J. Am. Chem. Soc.* **1986**, *108*, 5763–5771. (e) Yamaguchi, K.; Takahara, Y.; Fueno, T. In *Applied Quantum Chemistry*; Smith, V. H., Ed.; D. Riedel: Dordrecht, The Netherlands, 1986; p 155. (f) Soda, T.; Kitagawa, Y.; Onishi, T.; Takano, Y.;

- Shigeta, Y.; Nagao, H.; Yoshioka, Y.; Yamaguchi, K. *Chem. Phys. Lett.* **2000**, *319*, 223–230.
- (17) (a) Bhattacharya, D.; Misra, A. *J. Phys. Chem. A* **2009**, *113*, 5470–5475. (b) Shil, S.; Misra, A. *J. Phys. Chem. A* **2010**, *114*, 2022–2027. (c) Bhattacharya, D.; Shil, S.; Misra, A.; Klein, D. J. *Theor. Chem. Acc.* **2010**, *127*, 57–67. (d) Bhattacharya, D.; Shil, S.; Misra, A. *J. Photochem. Photobiol. A* **2011**, *217*, 402–410. (e) Saha, A.; Latif, I. A.; Datta, S. N. *J. Phys. Chem. A* **2011**, *115*, 1371–1379. (f) Atanasov, M.; Daul, C. A. *Chem. Phys. Lett.* **2008**, *381*, 584–591.
- (18) (a) Longuet-Higgins, H. C. *J. Chem. Phys.* **1950**, *18*, 265–274. (b) Higuichi, J. *J. Chem. Phys.* **1963**, *39*, 1847–1852. (c) Borden, W. T.; Davidson, E. R. *J. Am. Chem. Soc.* **1977**, *99*, 4587–4594. (d) Maynau, D.; Said, M.; Malerieu, J. P. *J. Am. Chem. Soc.* **1983**, *105*, 5244–5252. (e) Lloret, F.; Journaux, J. Y.; Julvela, M. *Inorg. Chem.* **1990**, *29*, 3967–3972. (f) Klein, D. J.; Nelin, C. J.; Alexander, S.; Matsen, F. A. *J. Chem. Phys.* **1982**, *77*, 3101–3108. (g) Barone, V.; Bencini, A.; di Matteo, A. *J. Am. Chem. Soc.* **1997**, *119*, 10831–10837.
- (19) Paul, S.; Misra, A. *J. Phys. Chem. A* **2010**, *114*, 6641–6647 and references therein.
- (20) McConnell, H. M. *J. Chem. Phys.* **1963**, *39*, 1910.
- (21) (a) Heitler, W.; London, F. Z. *Phys.* **1927**, *44*, 455–472. (b) Anderson, P. W. In *Magnetism*; Rado, G. T., Suhl, H., Eds.; Academic Press: New York, 1963.
- (22) Yoshizawa, K.; Yamabe, T.; Hoffmann, R. *Mol. Cryst. Liq. Cryst.* **1997**, *305*, 157–166.
- (23) Caballol, R.; Castell, O.; Illas, F.; de P. R. Moreira, I.; Malrieu, J. P. *J. Phys. Chem. A* **1997**, *101*, 7860–7866.
- (24) (a) Boiteaux, C. B.; Mouesca, J. M. *J. Am. Chem. Soc.* **2000**, *122*, 861–869. (b) Boiteaux, C. B.; Mouesca, J. M. *Theor. Chem. Acc.* **2000**, *104*, 257–264.
- (25) Ruiz, E.; Cano, J.; Alvarez, S.; Alemany, P. *J. Comput. Chem.* **1999**, *20*, 1391–1400.
- (26) (a) Mataga, N. *Theor. Chim. Acta* **1968**, *10*, 372–376. (b) Ovchinnikov, A. A. *Theor. Chim. Acta* **1978**, *47*, 297–304.
- (27) (a) Gao, E. Q.; Kui Tang, J.; Yan, S. P.; Liao, D. Z.; Jiang, Z. H. *Trans. Met. Chem.* **2001**, *26*, 473–476. (b) Ruiz, E.; Cirera, J.; Alvarez, S. *Coord. Chem. Rev.* **2005**, *249*, 2649–2660. (c) Paul, S.; Misra, A. *Inorg. Chem.* **2011**, *50*, 3234–3246.
- (28) (a) Kollmar, C.; Kahn, O. *Acc. Chem. Res.* **1993**, *26*, 259–265. (b) Yoshizawa, K.; Hoffmann, R. *J. Am. Chem. Soc.* **1995**, *117*, 6921–6926. (c) Tyutylkov, N.; Staneva, M.; Stoyanova, A.; Alaminova, D.; Olbrich, G.; Dietz, F. *J. Phys. Chem. B* **2002**, *106*, 2901–2909.
- (29) (a) Izouka, A.; Murata, S.; Sugawara, T.; Iwamura, H. *J. Am. Chem. Soc.* **1985**, *107*, 1786–1787. (b) Izouka, A.; Murata, S.; Sugawara, T.; Iwamura, H. *J. Am. Chem. Soc.* **1987**, *109*, 2631–2639. (c) Iwamura, H. *Adv. Phys. Org. Chem.* **1990**, *26*, 179–253.
- (30) (a) Yamaguchi, K.; Toyoda, Y.; Fueno, T. *Chem. Phys. Lett.* **1989**, *159*, 459–464. (b) Buchachenko, A. L. *Mol. Cryst. Liq. Cryst.* **1989**, *176*, 307–319.
- (31) (a) Deumal, M.; Novoa, J. J.; Bearpark, M. J.; Celani, P.; Olivucci, M.; Robb, M. A. *J. Phys. Chem. A* **1998**, *102*, 8404–8412. (b) Deumal, M.; Cirujeda, J.; Veciana, J.; Novoa, J. J. *Chem.—Eur. J.* **1999**, *5*, 1631–1642. (c) Novoa, J. J.; Deumal, M.; Lafuente, P.; Robb, M. A. *Mol. Cryst. Liq. Cryst.* **1999**, *335*, 603–612.
- (32) (a) Anderson, P. W. *Phys. Rev.* **1950**, *79*, 350–356. (b) Anderson, P. W. *Phys. Rev.* **1959**, *115*, 2–13. (c) Anderson, P. W. Theory of the Magnetic Interaction: Exchange in Insulators and Superconductors. In *Solid State Physics*; Turnbull, F., Seitz, F., Eds.; Academic Press: New York, 1963; Vol. 14, p 99.
- (33) (a) Desmaris, N.; Reuse, F. A.; Khanna, S. N. *J. Chem. Phys.* **2000**, *112*, 5576–5584 and references therein. (b) Negodaev, I.; de Graff, C.; Caballol, R. *Chem. Phys. Lett.* **2008**, *458*, 290–294. (c) Paul, S.; Misra, A. *THEOCHEM* **2009**, *907*, 35–40. (d) Mitra, S.; Mandal, A.; Datta, A.; Banerjee, S.; Chakravorty, D. *J. Phys. Chem. C* **2011**, *115*, 14673–14677.
- (34) Paul, S.; Misra, A. *THEOCHEM* **2009**, *895*, 156–160.
- (35) (a) Calzado, C. J.; Cabrero, J.; Malrieu, J. P.; Caballol, R. *J. Chem. Phys.* **2002**, *116*, 2728–2747. (b) Calzado, C. J.; Cabrero, J.; Malrieu, J. P.; Caballol, R. *J. Chem. Phys.* **2002**, *116*, 3985–4000.
- (c) Calzado, C. J.; Angeli, C.; Taratiel, D.; Caballol, R.; Malrieu, J. P. *J. Chem. Phys.* **2009**, *131*, 044327–044340.
- (36) (a) White, R. M. In *Quantum Theory of Magnetism*; Springer: New York, 2007. (b) Jorgensen, P.; Simons, J. In *Second Quantization Based Methods in Quantum Chemistry*, Academic Press, Inc.: New York, 1981.
- (37) Amos, A. T.; Hall, G. G. *Proc. R. Soc. London, Ser. A* **1961**, *263*, 483–493.
- (38) Kramers, H. A. *Physica* **1934**, *1*, 182–192.
- (39) Jordan, P.; Wigner, E. Z. *Phys.* **1928**, *47*, 631–651.
- (40) (a) McConnell, H. M. *J. Chem. Phys.* **1958**, *28*, 1188–1192. (b) Nakatsuji, H.; Hirao, K. *J. Chem. Phys.* **1978**, *68*, 4279–4291.
- (41) (a) Hart, J. R.; Rappe, A. K.; Goran, S. M.; Upton, T. H. *J. Phys. Chem.* **1992**, *96*, 6264–6269. (b) Kolczewski, C. H.; Fink, K.; Staemmler, V. *Int. J. Quantum Chem.* **2000**, *76*, 137–147. (c) Rimmer, D. E. *J. Phys. Chem. C* **1969**, *2*, 329–338.
- (42) Zhuldev, A.; Barone, V.; Bonnet, M.; Delley, B.; Grand, A.; Ressouche, E.; Rey, P.; Subra, R.; Schweizer, J. *J. Am. Chem. Soc.* **1994**, *116*, 2019–2027.
- (43) Frisch, M. J.; Trucks, G. W.; Schlegel, H. B.; Scuseria, G. E.; Robb, M. A.; Cheeseman, J. R.; Montgomery, J. A., Jr.; Vreven, T.; Kudin, K. N.; Burant, J. C.; Millam, J. M.; Iyengar, S. S.; Tomasi, J.; Barone, V.; Mennucci, B.; Cossi, M.; Scalmani, G.; Rega, N.; Petersson, G. A.; Nakatsuji, H.; Hada, M.; Ehara, M.; Toyota, K.; Fukuda, R.; Hasegawa, J.; Ishida, M.; Nakajima, T.; Honda, Y.; Kitao, O.; Nakai, H.; Klene, M.; Li, X.; Knox, J. E.; Hratchian, H. P.; Cross, J. B.; Bakken, V.; Adamo, C.; Jaramillo, J.; Gomperts, R.; Stratmann, R. E.; Yazyev, O.; Austin, A. J.; Cammi, R.; Pomelli, C.; Ochterski, J. W.; Ayala, P. Y.; Morokuma, K.; Voth, G. A.; Salvador, P.; Dannenberg, J. J.; Zakrzewski, V. G.; Dapprich, S.; Daniels, A. D.; Strain, M. C.; Farkas, O.; Malick, D. K.; Rabuck, A. D.; Raghavachari, K.; Foresman, J. B.; Ortiz, J. V.; Cui, Q.; Baboul, A. G.; Clifford, S.; Cioslowski, J.; Stefanov, B. B.; Liu, G.; Liashenko, A.; Piskorz, P.; Komaromi, I.; Martin, R. L.; Fox, D. J.; Keith, T.; Al-Laham, M. A.; Peng, C. Y.; Nanayakkara, A.; Challacombe, M.; Gill, P. M. W.; Johnson, B.; Chen, W.; Wong, M. W.; Gonzalez, C.; Pople, J. A. *Gaussian 03*, revision D.01; Gaussian Inc.: Wallingford, CT, 2004.
- (44) (a) Brook, D. J. R.; Fox, H. H.; Lynch, V.; Fox, M. A. *J. Phys. Chem.* **1996**, *100*, 2066–2071. (b) Tokii, T.; Hamamura, N.; Nakashima, M.; Muto, Y. *Bull. Chem. Soc. Jpn.* **1992**, *65*, 1214–1219. (c) Castillo, O.; Muga, I.; Luque, A.; Gutierrez-Zorrilla, J. M.; Sertucha, J.; Vitoria, P.; Roman, P. *Polyhedron* **1999**, *18*, 1235–1245.
- (45) Neese, F. *ORCA: An Ab Initio, Density Functional and Semiempirical Program Package*, version 2.6, revision 35, 2007; Institut fuer Physikalische und Theoretische Chemie, Universitaet Bonn: Bonn, Germany, 2006.
- (46) (a) Rudberg, E.; Satek, P.; Rinkevicius, Z.; Agren, H. *J. Chem. Theory Comput.* **2006**, *2*, 981–989. (b) Seal, P.; Chakrabarti, S. *J. Phys. Chem. A* **2008**, *112*, 3409–3413.
- (47) Shao, Y.; Head Gordon, M.; Krylov, A. *J. Chem. Phys.* **2003**, *118*, 4807–4818.
- (48) Wang, F.; Ziegler, T. *J. Chem. Phys.* **2004**, *121*, 12191–12196.
- (49) Yang, K.; Peverati, R.; Truhlar, D. G.; Valero, R. *J. Chem. Phys.* **2011**, *135*, 044118–044139.
- (50) (a) Valero, R.; Illas, F.; Truhlar, D. G. *J. Chem. Theory Comput.* **2011**, *7*, 3523–3531. (b) Zhekova, H.; Seth, M.; Ziegler, T. *J. Chem. Theory Comput.* **2011**, *7*, 1858–1866.
- (51) (a) Foster, J. P.; Weinhold, F. *J. Am. Chem. Soc.* **1980**, *102*, 7211–7218. (b) Carpenter, J. E. Extension of Lewis Structure Concepts to open shell and excited state molecular species. Ph. D. Thesis, University of Wisconsin, Madison, WI, 1987. (c) Reed, A. E.; Curtiss, L. A.; Weinhold, F. *Chem. Rev.* **1988**, *88*, 899–926. (d) Weinhold, F.; Carpenter, J. E. The structure of small molecules and ions. In *The Structure of Small Molecules and Ions*; Naamam, R., Vager, Z., Eds.; Plenum: New York, 1988; p 227.
- (52) Rudra, I.; Wu, Q.; Voorhis, T. V. *J. Chem. Phys.* **2006**, *124*, 024103.

(53) (a) Trindle, C.; Datta, S. N. *Int. J. Quantum Chem.* **1996**, *57*, 781–799. (b) Polo, V.; Alberola, A.; Andres, J.; Anthony, J.; Pilkington, M. *Phys. Chem. Chem. Phys.* **2008**, *10*, 857–864.

(54) Chevrau, H.; de P. R. Moreira, I.; Silvi, B.; Illas, F. J. *Phys. Chem. A* **2001**, *105*, 3570–3577.

(55) (a) Lahti, P. M. In *Design of Organic-Based Materials with Controlled Magnetic Properties*; Turnbull, M. M., Sugimoto, T., Thomposon, L. K., Eds.; American Chemical Society: Washington, DC, 1996; ACS Symposium Series 664. (b) Rajca, A. *Chem. Rev.* **1994**, *94*, 871–893. (c) Dougherty, D. A. *Acc. Chem. Res.* **1991**, *24*, 88–94. (d) Novoa, J. J.; Mota, F.; Veciana, J.; Cirujeda, J. *Mol. Cryst. Liq. Cryst.* **1995**, *271*, 79–90.